Pure Appl. Geophys. 169 (2012), 769–781

DOI 10.1007/s00024-011-0334-y

Pure and Applied Geophysics

Use of a Sodar to Improve the Forecast of Fogs and Low Clouds on Airports

Alain Dabas,[1] Samuel Remy,[2] and Thierry Bergot[1]

Abstract—A sodar was deployed at Roissy–Charles de Gaulle airport near Paris, France, in 2008 with the aim of improving the forecast of low visibility conditions there. During the winter of 2008–2009, an experiment was conducted that showed that the sodar can effectively detect and locate the top of fog layers which is signaled by a strong peak of acoustic reflectivity. The peak is generated by turbulence activity in the inversion layer that contrasts sharply with the low reflectivity recorded in the fog layer below. A specific version of the 1D-forecast model deployed at Roissy for low visibility conditions (COBEL-ISBA) was developed in which fogs' thicknesses are initialized by the sodar measurements rather than the information derived from the down-welling IR fluxes observed on the site. It was tested on data archived during the winters of 2008–2009 and 2009–2010 and compared to the version of the model presently operational. The results show a significant improvement—dissipation times of fogs are better predicted.

1. Introduction

The prediction of low visibility conditions is a formidable challenge for operational weather forecast services. Adverse visibility conditions can strongly reduce the efficiency of a terminal area traffic flow. At Paris—Charles de Gaulle (CDG) international airport, Low Visibility Procedures (LVP) are applied when visibility is under 600 m (2,000 feet) or the ceiling is below 60 m (200 feet). The application of LVP reduces airport efficiency for takeoffs and landings by a factor of two. Costly delays and flight cancellations ensue. CDG is the largest airport in France and was number 2 in 2009 in Europe for the number of passengers. It is a hub for AirFrance-KLM and, as such, receives many passengers connecting from one flight to another. It is strongly affected by fogs during a significant amount of time every year. Owing to its importance at the national and European level, CDG was equipped with a specific system for the prediction of low-visibility conditions. The system is based on the 1D COBEL-ISBA numerical model and a dedicated observation package (see Bergot *et al.* 2005 and Bergot, 2007 for a detailed description). The high resolution 1D COBEL-ISBA model was developed in collaboration between the Laboratoire d'Aérologie (Université Paul Sabatier/CNRS, Toulouse, France) and the Centre National de Recherches Météorologique (Météo-France/CNRS, Toulouse, France). A detailed description of the model can be found in Bergot and Guedalia, (1994). The COBEL equations are solved on a high-resolution vertical grid. Near the surface, in the region of significance for fog, numerical computations are made on a very fine mesh grid (20 vertical levels in the first 200 m, with a first level at 0.5 m). The physical package includes a parameterization of boundary layer turbulent mixing for stable, neutral and unstable conditions, a microphysical parameterization adapted for fogs and low clouds and a detailed radiation transfer scheme. The COBEL atmospheric model is coupled with the ISBA seven layer surface scheme (Noilhan and Planton, 1989).

Accurate short-term forecasting of fogs and low clouds strongly depends on the accuracy of initial conditions (Remy and Bergot, 2009). Specific observations are made at CDG in order to improve the description of the surface boundary layer. Atmospheric temperature and humidity profiles, as well as short- and long-wave radiation fluxes, are performed on a 30 m high meteorological tower (levels of measurements: 1, 2, 5, 10 and 30 m). These observations are used in a local assimilation scheme (see Bergot *et al.* 2005 for details, only a brief

[1] CNRM-GAME, 42 Av Coriolis, 31057 Toulouse Cedex, France. E-mail: alain.dabas@meteo.fr

[2] Météo-France Direction Ile de France Centre, 2 Av Rapp, 75340 Paris Cedex07, France.

description will be given hereafter). The assimilation process is done in three steps:

- assimilation of atmospheric profiles: local observations, forecast from the French numerical weather prediction (NWP) model ALADIN and the guess profiles are mixed following a classical BLUE equation (Best Linear Unbiased Estimator). The error statistics are imposed in order that the initial profiles are close to observations near the surface and get closer to the NWP forecast at the top of the model.
- Assimilation of fog and low cloud layers: the atmospheric profiles inside the fog layer are adjusted following the hypothesis that the cloudy layer is well-mixed. The fog depth is determined using an iterative method that minimizes the model error on radiation fluxes.
- Assimilation of soil profiles: the temperature and moisture profiles inside the soil are linearly interpolated from in situ measurements.

The second step of assimilation, i.e. the initialization of the fog layer, is very important for an accurate forecast of the dissipation of the fog layer. When the fog layer is between the two levels of the down-welling IR radiation measurements (at Roissy CDG, the radiation sensors are at ground and at 45 m above the surface), the minimization of radiation fluxes divergence between the two levels allows an accurate initialization of the fog layer (see Bergot *et al.* 2005 for details). However, when the top of the fog layer is above the highest sensor, the divergence between the two sensors is null and the estimation of the fog layer height is then more difficult. The errors in the measurements of radiation fluxes due, in particular, to the deposition of droplets on the sensor window lead to errors in the fog height that can be up to several tens of meters. Another source of error is the possible presence of a cloud layer above the fog that produces a stronger down-welling IR flux that the model interprets as a fog layer thicker than it is in reality. The goal of this article is to test how the use of sodar measurements can help the initialization of fog layers (instead of the use of radiation profiles). The first section is devoted to the sodar and the possibility of using this instrument for detecting the top of fog layers. Results of an experiment conducted in the winter of 2008–2009 at Roissy CDG are presented. Then, in Sect. 4, the impact of sodar detected fog top data on the forecast of LVP conditions by COBEL-ISBA at CDG is studied.

2. Sodar

2.1. The Sodar Technology

Acoustic sounders, or sodars, have been widely used since the 1970s for observing the atmospheric boundary layer (see review paper by Coulter and Kallistratova, 2004). Benefiting from several decades of development, sodar technology has reached a high degree of maturity. Today, fully automatic sodars, able to operate unattended for long time periods with minimal maintenance, are available off the shelf from several manufacturers at prices below 100 k€.

A sodar probes the atmosphere by emitting pulsed sound waves. While it propagates, the sound wave is backscattered by turbulent temperature heterogeneities. The small fraction of the emitted sound power thus scattered back to the sodar is detected by microphones and analyzed. The strength P_r of the backscattered sound is given by the sodar equation (Little, 1969)

$$P_r(r) = PA\frac{c\tau}{2}\frac{\sigma(r)L(r)}{r^2} \qquad (1)$$

It is proportional the power P (W) of the emitted sound, the pulse duration τ (s), the receiver "efficiency" A (m^2) and the celerity of sound c (ms^{-1}). It is a function of the range r (m) through the $1/r^2$ term, the round-trip transmission factor $L(r)$ (which decreases with the range r) and the backscattering coefficient $\sigma(r)$ of the atmosphere. This latter parameter characterizes the "reflective" power of the atmosphere; it is related to its thermodynamic properties

$$\sigma(r) = 0.0039\,k^{\frac{1}{3}}\,C_\tau^2(r)/T^2(r) \qquad (2)$$

Here, $k = 2\pi/\lambda$ is the wavenumber (λ (m) is the wavelength—typically of the order of 10 cm), $C_\tau^2(r)$ ($K^2\ m^{2/3}$) is the structure coefficient of the temperature turbulence, and $T(r)$ (K) is the absolute temperature.

The most common application of a sodar is the measurement of highly resolved, vertical profiles of

wind within the first several hundreds of meters of the atmosphere. This application is based on the estimation of the frequency Doppler shift δf (Hz) between the outgoing and the backscattered sound waves. It is proportional to the wind velocity component v_r along the sodar beam

$$\delta f = -\frac{2v_r}{\lambda} \tag{3}$$

Combining at least 3 beam directions (with 3 different antennas, or a phased-array antenna), it is then possible to retrieve vertical profiles of the 3D wind vector. In comparison to other wind profiling systems (lidar or UHF radar), a sodar offers the advantage of a fine time and space resolution (a few minutes and several tens of meters in the vertical direction) but limited ranges (the transmission factor $L(r)$ decreases rapidly with the range).

In the present article, the sodar is used for real-time detection of the top of fog layers. Although several papers report sodar observations of stable boundary layers—see for instance GUÉDALIA *et al.* 1980, or ANDERSON, 2003—this is an unusual application (to our knowledge). An enhanced turbulent activity is expected at the top of the fog layers due to radiative cooling and wind shear. Therefore, sodar backscatter at the top of a fog layer is stronger than above or below. It must be noted here that the fine time and space resolutions of a sodar are particularly well suited to the observation of fogs which are thin (the typical thicknesses of fogs is several tens to several hundreds of meters) and evolve at time scales of several minutes.

2.2. *Instrumental Set-up*

The ability of a sodar to detect the top of fog layers was tested during an experiment conducted by the Groupe d'Étude de l'Atmosphère Météorologique (a research laboratory operated by the French weather service Météo-France and the Centre National de la Recherche Scientifique, the main research operator in France) during the winter of 2008–2009. It took place at Roissy Charles de Gaulle (CDG) airport.

The experimental set-up was composed of a sodar PCS.2000-64 from METEK (see details below), a tethered balloon, and a ceilometer. It was complemented by various observation systems operated routinely at the airport (including 12 visibility sensors DF320 from DEGREANE, and 4 ceilometers LD-WHX05 from IMPULSPHYSICS).

The sodar was deployed in the summer of 2008 (see Fig. 1) at a location (see Fig. 2) carefully selected after measurements of ambient acoustic noise at different possible places in the airport area. The site is in the western, restricted area of the airport, and in the axis of the two runways 09R and 09L forming the northern "doublet" of CDG. The distance to the runways is 700 and 1,950 m respectively. There, the ambient noise can peak high above 100 dBa when an aircraft lands or takes-off, which happens once every 90 s during rush hours, but it is otherwise surprisingly low—below 45 dBa. The calm periods between aircraft noise peaks last long enough (about 70 s) to allow the sodar to make reliable measurements (the sodar software is able to discard noisy signals from the wind and the reflectivity retrieval process). The main characteristics of the sodar are listed in Table 1, while Table 2 shows the instrument parameters set by METEK for the experiment. The antenna was a phased array of $8 \times 8 = 64$ transducers. It was divided into 4 sub-panels. Independent 90° phase delays can be added to each sub-panel so that the sodar can emit beams in up to 5 different directions, one of them the vertical (all sub-panels are in phase), the other four pointing $\sim$20° off-zenith and at 90° azimuth increments. In practice, only 3 directions were used (vertical and two of the four titled directions, the last two being redundant and affected by echoes from nearby towers). The sodar was parameterized so as to achieve the best possible vertical resolution (10 m) and a first range gate as low as possible (bottom altitude at 15 m). The integration time was set to 10 min as no major fog evolutions were expected during so short a time period. As for the maximum altitude (350 m), the requirement was based on a climatology study according to which most fogs at CDG (75%) do not exceed 100 m in thickness. It was raised to 460 m after the experiment (from October 2009) as sodar data showed the study had probably underestimated the occurrence of thick fogs.

The tethered balloon system was aimed at measuring vertical profiles of temperature and humidity at the high repetition rate of 1 or 2 per hour. It served as the reference for the altitude of fog layer tops that are marked by a thermal inversion and a sudden drop in the relative humidity. For safety reasons, the tethered balloon could not be deployed close to the sodar, but was located 7 km away to north of the airport. Another constraint was that the maximum balloon altitude was limited to about 300 m above the surface. As the topography around the airport is rather flat and homogeneous (the terrain slope is $\sim 0.13°$, the sodar being only 16 m below the balloon sounding system), it was expected that the fogs at CDG would be rather horizontally homogeneous, in particular when caused by radiative cooling, but differences between balloon and sodar fog top altitudes could be partly due to the distance between the two instruments.

The tethered balloon system was composed of a winch TTW111 (see Fig. 3), an SPS220 sonde receiver and a DIGICORA III processing system, all from Vaisala. The sondes were standard RS92SGP from the same manufacturer, but placed in a home-made ventilating shield that was developed in order to compensate for the lack of natural ventilation of the sensing elements (in standard radiosounding, the ascending speed of $\sim 5\ \mathrm{ms}^{-1}$ naturally ventilates the sensors; with the tethered balloon, the ascending speed was only $\sim 0.5\ \mathrm{ms}^{-1}$). Vertical profiles of temperature and relative humidity were measured at the rate of 1 or 2 profiles per hour by letting the helium inflated balloon go up to the maximum altitude and then bringing it down to the surface with the winch. Ascents and descents lasted 15–30 min depending on winch speed. The sounding system was activated every time a fog event was predicted by the local station of Météo-France (the French weather service) or when an unexpected fog was observed at the airport. The purpose was to start the measurements 1 or 2 h before the formation of fog and to make vertical profiles of the atmosphere at regular time intervals until it disappeared. The sonde in operation was replaced every 2 to 3 h as the first nights of operation showed a saturation effect on the humidity sensor after a few hours. An example of a set of temperature and humidity profiles measured during a fog event is given in Fig. 4. The top of the fog layer is indicated by the sharp temperature increase and the correlated drop of humidity. In this

Figure 1
Picture of the sodar METEK PCS2000-64 deployed at Roissy CDG airport. The sodar antenna is *inside the white shield* in the middle of the picture. The shield is made of 4 vertical panels aimed at protecting the receiver from ambient noise

Figure 2
Satellite view of Roissy Charles de Gaulle airport with the position of the sodar west of the two runways forming the northern "doublet" of the airport. The distance to runway 09R is 700 m, and 1,950 m to runway 09L

Table 1

Main characteristics of the sodar PCS.2000-64 from METEK

Overall characteristics	
Frequency	~1,600 Hz
Wavelength	~21 cm
Emitted power	118 dbA and 50 W
Power consumption	
Without heater	250 W
With heater	550 W
Antenna	
Number of transducers	$8 \times 8 = 64$
Dimension	110×110 m
Weight	136 kg
Number of beam directions	Up to 5
Beam angles (nadir)	$0 \pm 22°$
Beam angles (azimuth)	0, 90, 180 and 270°
Measurement range	
Max horiz. velocity	30 ms^{-1}
Max vertical velocity	± 10 ms^{-1}
Number of range gates	40 max
Vertical resolution	5–100 m
Integration time	10–1,800 s
Precision	
Horizontal velocity	10%
Vertical velocity	5%
Direction	5°
Operating conditions	
Temperature	−30 to 45°C
Humidity	5–100%

Table 2

Sodar settings during the experiment conducted in the winter 2008–2009

Sodar settings	
Number of frequencies	1
Number of beam directions	3
Base altitude of lowest range gate	15 m
Nbre of range gates	34
Top altitude of highest range gate	360 m
Vertical resolution	10 m
Integration time	10 min

particular case (7th of December, 2008, at 12:20 UTC), its altitude was 250 m above sea-level.

The ceilometer was a CT25K from Vaisala. It was deployed at the local station of Météo-France (indicated by CDM95 in Fig. 2). It is a small backscatter lidar that operates in the near IR at 0.9 μm. It produces two types of messages. The most common contains the height of cloud bottoms. During the experiment, we were mostly interested by the second type, which contains lidar backscatter signals. As shown in Fig. 5, the presence of a fog is signaled by a strong return at the surface (the small water droplets in the fog strongly reflect the light emitted by the lidar) followed

Figure 3
Picture of the sounding system used during the experiment of 2008–2009. A standard radiosounding balloon with a radiosonde RS92SGP mounted in a home-made ventilating shield is tied to the electric winch. During fogs, the balloon and the sonde were allowed to go up and brought back one or two times every hour

by a steep attenuation (the strong scattering attenuates the laser beam very steeply). It must be stressed here that the thickness of the return is in no way related to the thickness of the fog; it is a function of the laser pulse length (15 m in the present case) and the multiple scattering effect (many photons captured by the ceilometers were scattered several times by several particles—see for instance Bissonnette *et al.* (1995), for details on multiple scattering effects on lidar returns). During the experiment, we used ceilometer returns in order to determine precisely the time

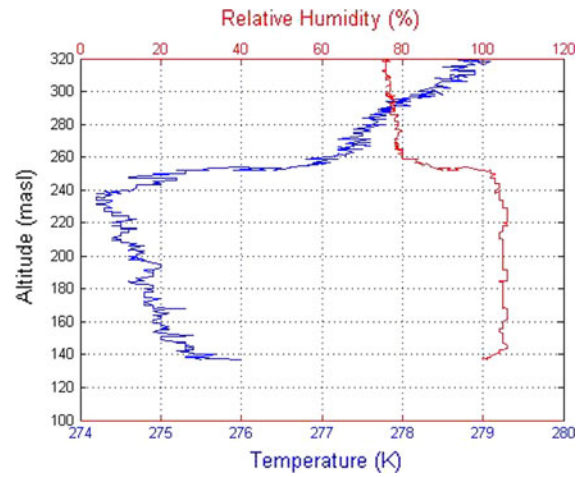

Figure 4
Temperature (*blue*) and relative humidity (*red*) profiles measured by the tethered balloon on the 7th of December 2008 at 12:20 UTC. The top of the fog layer (*black dashed line*) appears very clearly at the altitude of 250 m with the sharp increase of temperature and the drop of the relative humidity. Note that the humidity sensor is oversaturated in the fog layer and measures a relative humidity of ~105%

of fog formation and dissipation (see the following section).

3. Data Analysis

Eleven observation periods were carried out during the campaign. During seven of them, a fog event was actually observed. For the other four, the fog prediction turned out to be a false alarm.

Figure 5 is a typical example of the observations acquired by the various sensors during a fog event. The particular event portrayed by the figure lasted a little more than 24 h, from 10:00 UTC on the 7th of December 2008 to 10:00 UTC on the 8th of December. The top graph contains the visibility (blue line) and cloud ceiling (red line) measured by airport sensors close to the sodar. At 10 UTC on the 7th of December, the visibility drops below 1,000 m indicating the sudden formation of a fog at CDG. The suddenness of the formation is clear on ceilometer data (bottom graph) where a strong lidar reflectivity appears almost instantly at the surface. The fog lasts until 10:00 UTC the next day, but a temporal dissipation at the surface occurs between 18:00 UTC and 24:00 UTC on the 7th

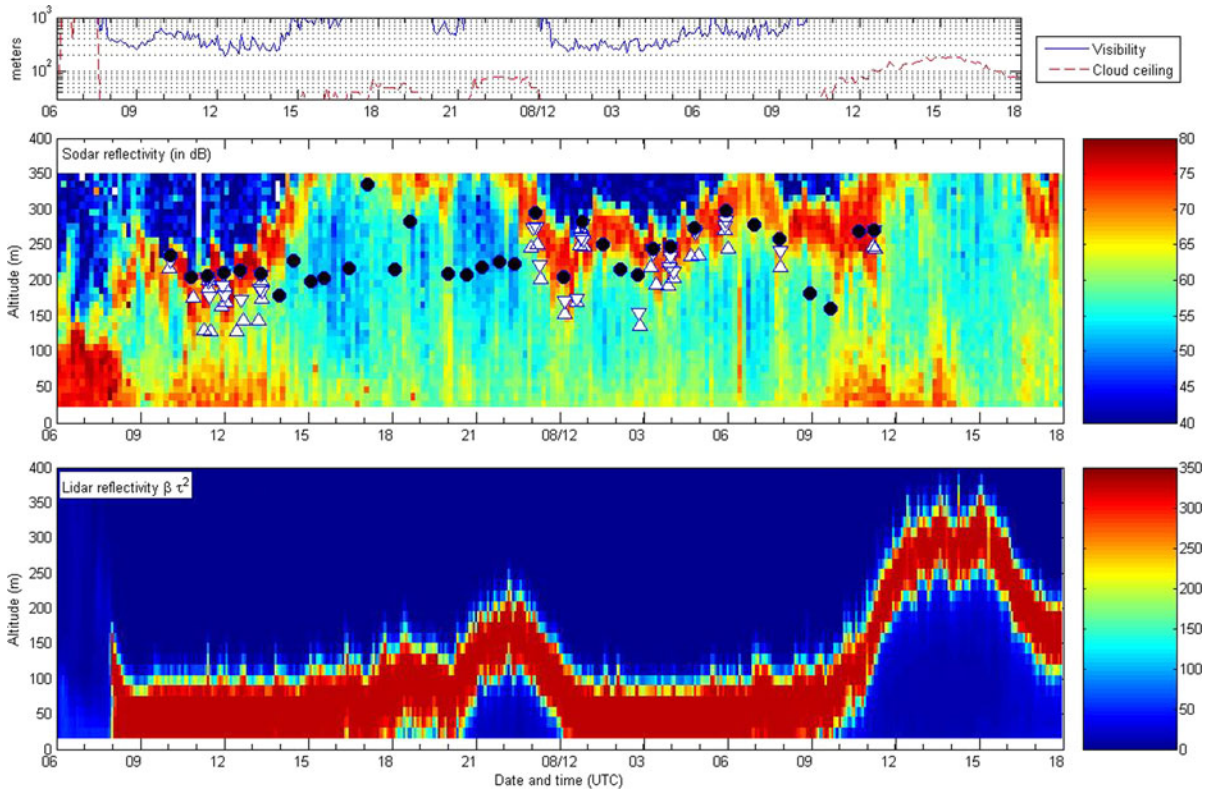

Figure 5

Visibility, cloud ceiling (*top*), sodar reflectivity (*middle*) and lidar reflectivity (*bottom*) measured from 6:00 UTC on 7th of December 2008 to 18:00 UTC on 8th of December 2008. Strong lidar reflectivities at the surface indicate the presence of fog. The fog event started suddenly at 8:00 UTC on December 7th. The dissipation occurred the next day at about 10:00 UTC. On the evening of the 7th, the fog dissipated temporally at the surface between 18:00 UTC and 24:00 UTC. Then the visibility reached over 1,000 m, but the cloud ceiling remained very low. Low visibility procedures were activated when the visibility was below 600 m or the cloud ceiling below 200 ft, thus remained in effect during the whole period. On the sodar plot (*middle graph*), a thin, *red layer* of strong acoustic reflectivities can be seen during the whole event. It is tightly correlated to the temperature inversions detected on the balloon soundings and shown with Δ (*bottom of inversions*) and ∇ (*top of inversions*). The *black spots* show the maximum altitude reached by the balloon. No inversion was detected on soundings with a maximum altitude below the red sodar reflectivity layer

of December. During this period, the visibility exceeds 1,000 m, but the cloud ceiling remains very low. Low visibility procedures were thus maintained at the airport throughout the whole period. Sodar reflectivities are displayed in the middle graph in dB units. At the time the fog forms, the strong reflectivity above the surface drops, and a thin layer of strong acoustic reflectivity (red) appears at the height of about 200 m. The layer remains during the whole fog period. Its height varies, ascends beyond the sodar maximum range (360 m) during the afternoon of 7 December, and then descends and stabilizes at about 250 m until dissipation. This layer contrasts sharply with the low reflectivity ($\lesssim$55 db) at the lower heights. The temperature inversions detected manually (that is by a visual inspection) on the balloon profiles are shown with white triangles pointing up (bottom of the inversion) or down (top of the inversion). The gradient at the inversion is typically of the order of 0.01 km^{-1}. The inversions are tightly correlated with the peak sodar reflectivities. This and the absence of temperature inversions on the profiles that did not reach the red layer (the maximum altitude of balloon profiles are indicated with black spots) suggest that strong sodar reflectivities during fogs are indeed a good signature of the presence of a fog top temperature inversion.

The correlation between the altitude of peak sodar reflectivity during fogs and the altitude of detected

inversions was extended to the 7 fog events documented during the experiment. The result is summarized with a scatter plot in Fig. 6. The altitudes of the base and the top of inversions are distinguished by the use of two different markers (Δ: base, and ∇: top). The correlation coefficients are nearly 70% for both, with inversion tops 8 m above sodar peaks on the average, and inversion bottoms −27 m below. This confirms that there is a good correlation between peak sodar reflectivities and the tops of fog layers. Differences between the altitudes of both may reach several tens of meters on some occasions. Their significance is hard to assess. They are partly due to the difficulty of detecting inversion layers on some balloon profiles (the thermal inversion is sometime very small, less than 0.5 K), and could also be due to the distance between the sodar and the balloon. On some occasions, it appeared, for instance, that the fog was present at the balloon site several tens of minutes before the sodar, and vice versa. Considering these sources of uncertainty, the correlation coefficient reached here seems good enough to conclude that the sodar provides a reliable estimation of the top level of fog layers.

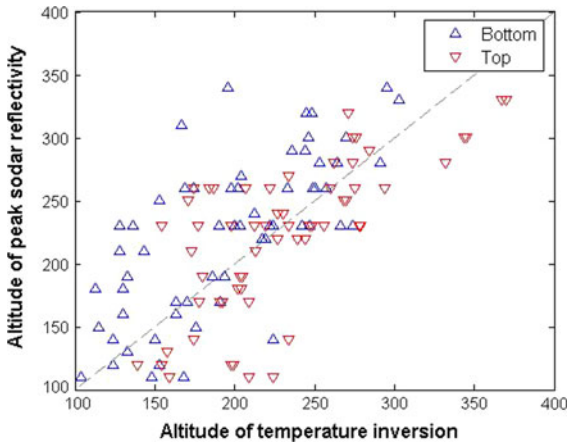

Figure 6
Scatter plot of peak sodar reflectivity altitudes versus temperature inversion altitudes. Top and bottom altitudes of temperature inversions are distinguished with *triangles* pointing *up* (*bottom*) and *down* (*top*). The number of temperature inversion tops is 60. On the average, they are 8 m above the sodar reflectivity peak (230 vs. 222 m). The correlation coefficient between inversions tops and sodar reflectivity peaks is 69.97%. As far as inversion bottoms are concerned (61 values), they are −27 m below sodar reflectivity peaks on the average (195 against 223 m) with a correlation coefficient of 69.44%

4. The Impact of Sodar Data on The COBEL-ISBA Forecasting System

The sodar data was used in the COBEL-ISBA forecasting system in order to check whether the forecasts of LVP conditions were improved or not.

4.1. Experimental setup

When fog was present at initialization time, the height of the fog layer provided by the sodar was used directly to initialize the liquid water content, with a value of 0.2 g/kg for the liquid water mixing ratio within the cloud. When stratus (i.e. a cloud with a base that is not touching the ground) was present, observations of the radiative fluxes were used as in the operational setup. As shown above, the sodar provided reliable estimates of the height of the top of a fog layer; however it has not been tested yet for stratus clouds.

The period of study covered 9 months from two successive winters: from 1 November 2008 to 28 February 2009 and from 1 October 2009 to 28 February 2010. LVP conditions were observed during 470 h during these two periods; they occurred more frequently during the early morning hours (local time is UTC plus 1 h during winter), as shown by Fig. 7. Overall, half of the LVP conditions were caused by fogs. Simulations were carried out at 1 h intervals: the model was run 6,492 times in total. The sodar observations were available for every simulation with fog at initialization time except one: the sodar was very reliable during the period of study (the average data availability has been larger than 95% until now, that is, after more than 2 years of operation).

The quality of the forecasts of LVP conditions was assessed in terms of Hit Ratio (HR) and pseudo-False Alarm Ratio (pseudo-FAR). When studying rare events, such as fog and LVP conditions, the pseudo-FAR is convenient because it removes the impact of the "no–no good forecasts" (no LVP forecast and no LVP observed), which mostly dominate the data sample and hide the true merits of the LVP forecast system. If a is the number of events forecasted and observed, b the number of events forecasted but not observed, and c the number

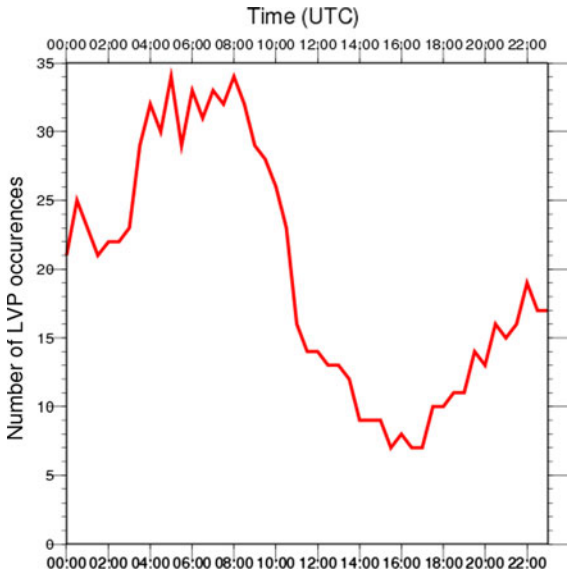

Figure 7
Number of occurrences of LVP conditions, depending on time of the day, from 1 November 2008 to 28 February 2009 and from 1 October 2009 to 28 February 2010

of events observed but not forecasted, HR and pseudo-FAR are then defined as follows:

$$HR = \frac{a}{a+c}; \quad pseudoFAR = \frac{b}{a+b} \qquad (4)$$

5. Results

Figure 8 shows the HR and pseudo-FAR of LVP conditions versus forecast time for simulations with the operational setup and with the use of sodar estimates of the thickness of the fog layer. A Student test for correlated samples was carried out to assess the significance level of the differences between the two experiments: its results are also shown in Fig. 8. The HR was higher when using sodar data as compared to the operational setup, with an increasing improvement for higher forecast times. This increase in the HR has a 95% significance level or above for forecast times larger than 1 h. The HR of LVP conditions for all simulations and forecast times was 0.585 with the sodar against 0.556 with the operational setup. The pseudo FAR was slightly degraded for forecast times below 2 h and slightly improved for higher forecast times, with a significance level over 95% for forecast times larger than 1 h. The overall pseudo FAR was 0.439 with the sodar against 0.443 with operational setup.

These statistics cover many cases for which the sodar data were not used, such as LVP due to stratus, or due to fogs that appear after initialization time. Figure 9 shows the HR and Pseudo-FAR of LVP conditions computed for simulations with a fog present at initialization time. A Student test was also carried out to check the significance level of the differences between the two experiments. The figure gives a better assessment of the impact of the sodar on fog predictions. A total of 263 h of LVP conditions correspond to these situations. The HR is improved for forecast times higher than 3 h, with an improvement larger for forecast times of 5 h and beyond. The pseudo-FAR follow the same pattern, with an important improvement for forecast times larger than 5 h. The differences were significant for forecast hours larger than 1 h for the HR and 3.5 h for the pseudo-FAR. It can thus be concluded that the sodar clearly improves the initialization of fogs in COBEL.

Figure 10 shows the compared statistics of both experiments for the forecast of the end time of LVP conditions, for simulations with fog at initialization time. The standard deviation of the forecast errors is slightly reduced when using the sodar, while the bias is slightly increased. 43% of simulations show an error smaller than 30 min when using the sodar, up to 40% with the operational setup. The bias difference between the two experiments was assessed to be significant with a level close to 100%, using a correlated samples Student test.

The initial fog thickness given by the sodar and the operational setup were compared in Fig. 11. When the operational setup gives values below 100 m, the sodar data are larger in nearly 80% of the cases. This could explain the better HR scores when using the sodar, as a thicker fog at initialization time lasts longer during the simulation. On the other hand, the validity of sodar data when the fog is thin is not very well known. The turbulence activity is generally stronger in the first tens of meters of the atmosphere, so the detection of a reflectivity peak due to the inversion at the top of

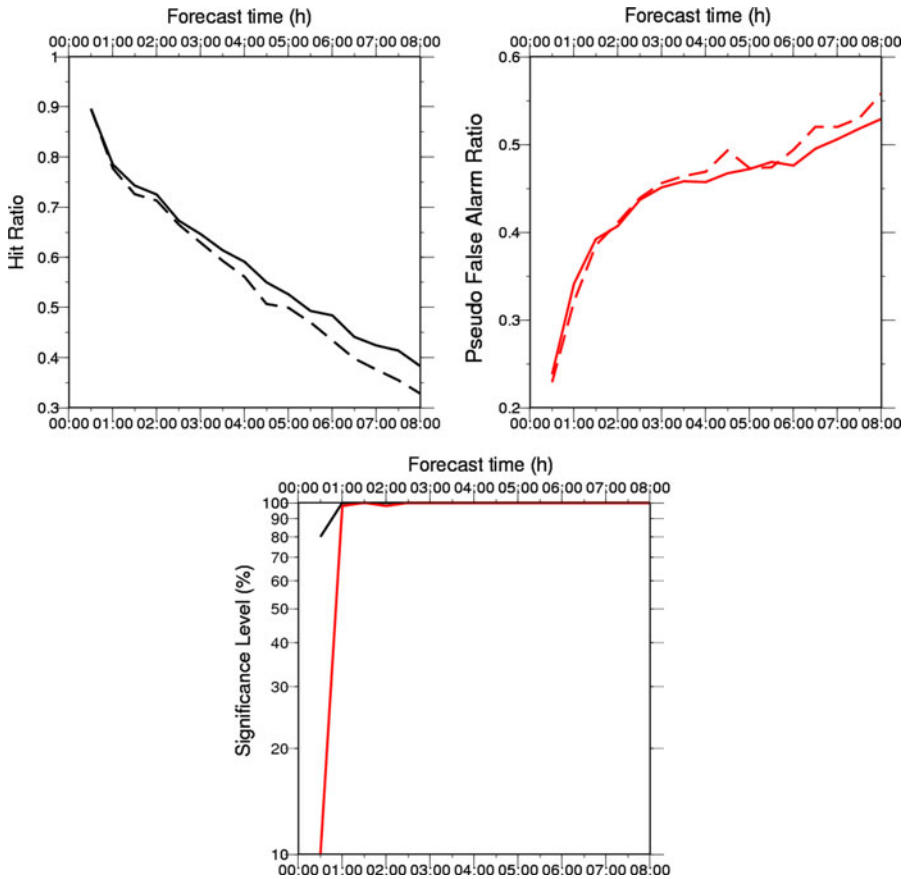

Figure 8
Hit Ratio (*top left*) and Pseudo-False Alarm Ratio (*top right*) versus forecast time. Simulations with the operational setup (*dashed line*) and using the sodar (*continuous line*), for the winters 2008–2009 and 2009–2010. The significance level for the difference between the operational setup and using the sodar is given in the *bottom*, for the Hit Ratio (*black*) and the Pseudo-False Alarm Ratio (*red*)

the fog is more difficult to detect. On the contrary, when the operational setup gives values between 100 and 300 m, no clear tendency can be drawn. For values above 300 m, the sodar data are always equal or lower, partly because of the range limit, but also partly because the operational set-up is sometimes misled by the presence of cloud above the fog layer.

6. Conclusions

The experiment conducted at CDG during the winter of 2008–2009 has proven that a sodar can operate efficiently at an airport to provide reliable measurements of the thickness of fog layers. Using sodar information (instead of down-welling IR fluxes) in the COBEL-ISBA model improved its hits and misses on low-visibility forecasts. In particular, the time of fog dissipation is better predicted. Part of the improvement is due to the enhanced data availability—nearly 1/3 of IR flux measurements are not available at the time of COBEL run while the average monthly availability of sodar data is better than 95%—but other problems, such as the presence of a stratus layer above the fog that led to errors in the estimates of the fog thickness using IR flux measurements and simulations, may be solved by the sodar. Future works will focus on a detailed understanding of the results that have been obtained;

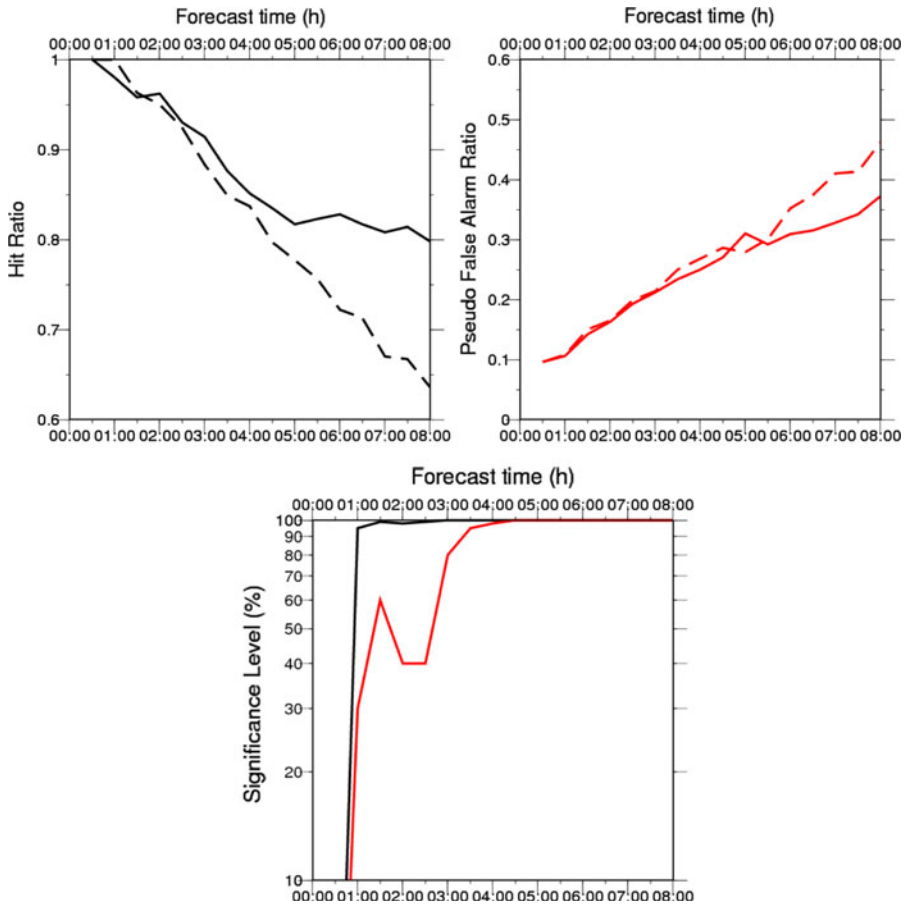

Figure 9
Same as Fig. 8 for simulations with fog at initialization time

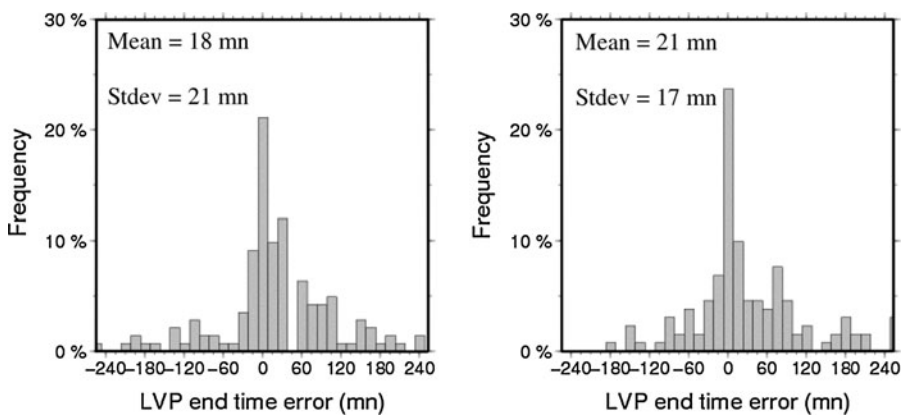

Figure 10
Frequency distribution histogram of the error of the predicted end time of LVP conditions, in minutes. The operational setup is on the *left*, simulations using the sodar data are on the *right*. Positive values correspond to a forecast of onset or end time that is too late. Errors larger than 240 min are grouped in the 240 min column. The mean and standard deviation of errors smaller than 240 min are indicated. The statistics were computed only for simulations with fog at initialization time

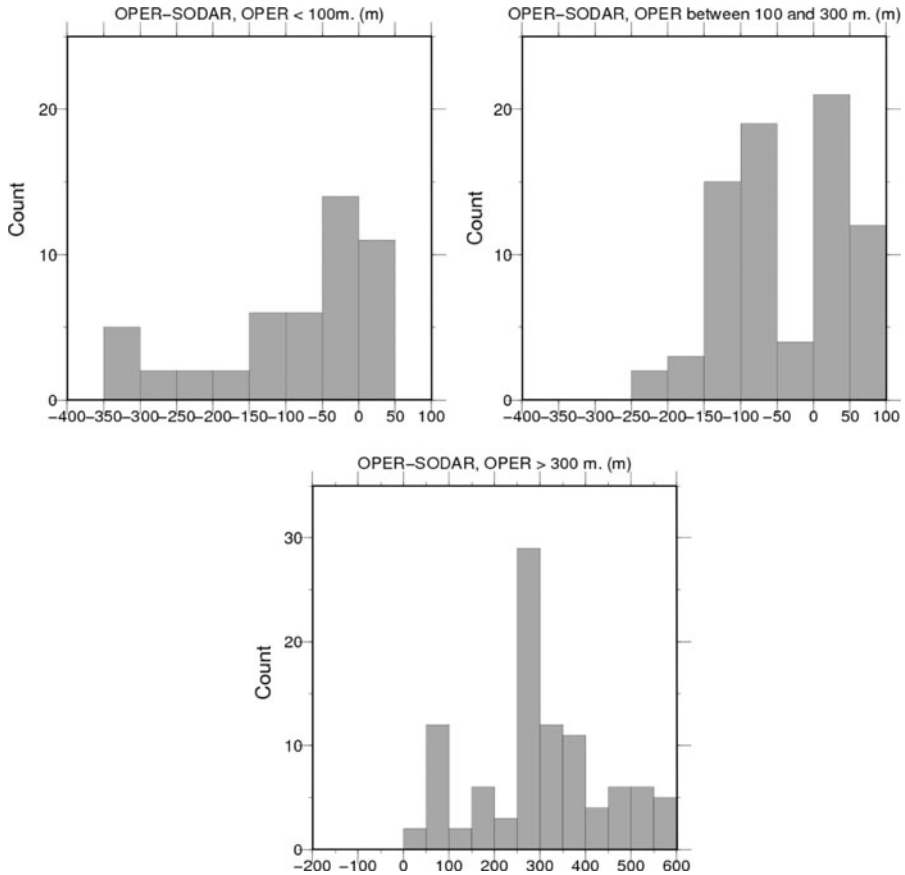

Figure 11
Fog thickness estimates using IR observations and simulations minus estimates by the sodar for thickness (as provided by the operational setup) below 100 m (*upper left*), between 100 and 300 m (*upper right*) and above 300 m (*bottom*)

in particular, they will aim at providing an explanation as to why some sodar estimations differ significantly from estimates using IR flux observations.

Acknowledgment

The work presented in this paper was financed by Météo-France. It is the fruit of the work of many people, in particular the people who spent long hours on cold nights operating the tethered balloon. We thank J.M. Donier, T. Douffet, F. Lavie, M. Olivier, O. Garrouste, O. Legain, A. Minisini, E. Moulin, G. Bouhours, D. Suquia, and J. Barrié. We also thank the staff of the local station of Météo-France (the Centre Départemental de la Météorologie 95) for their help.

References

Anderson, PS. (2003), *Fine-scale structure observed in a stable atmospheric boundary layer by sodar and kite-borne tethersonde*, Boundary Layer Meteorology *107*, 323–350.

Bergot T. (2007), *Quality Assessment of the Cobel-Isba numerical forecast system of fog and low clouds*, Pure appl. Geophys. *164*, 1265–1282.

Bergot, T. and Guedalia, D. (1994), *Numerical forecasting of radiation fog. Part I : Numerical model and sensitivity tests*, Mon. Wea. Rev. *122*, 1218–1230.

Bergot, T., Carrer, D., Noilhan, J. and Bougeault, P. (2005), *Improved site-specific numerical prediction of fog and low clouds : a feasibility study*, Weather and Forecasting *20*, 627–646.

Bissonnette, L. R., Bruscaglioni, P., Ismaelli, A., Zaccanti, G., Cohen, A., Benayahu, Y., Kleiman, M., Egert, S., Flesia, C., Schwendimann, P., Starkov, A.V., Noormohammadian, M., Oppel, U.G., Winker, M., Zege, E.P., Katsev, I.L. and Polonsky, I.N. (1995), *LIDAR multiple scattering from clouds*, Applied Physics B. *60*, 355–362.

Coulter R.L. and Kallistratova, M. A. (2004) *Two decades of progress in sodar techniques: a review of 11 ISARS proceedings*, Meteorol Atmos Phys. *85*, 3–19.

GUÉDALIA, D., NTSILA, A., DRUILHET, A. and FONTAN, J. (1980), *Monitoring of the atmospheric stability above urban and sub-urban site using sodar and radon measurements*, Journal of Applied Meotorology *19*, 839–848.

LITTLE, C.G. (1969), *Acoustic methods for the remote probing of the lower atmosphere*, Proc. IEEE. *57*, 571–578.

NOILHAN, J. and PLANTON, S. (1989), *A simple parametrization of land surface processes for meteorological models*, Monthly Weather Review A., *117*, 536–549.

REMY, S. and BERGOT, T. (2009), *Assessing the impact of observations on a local numerical fog prediction system*, Quarterly Journal of the Royal Meteorology *135*, 1248–1265.

(Received December 1, 2010, revised March 25, 2011, accepted April 8, 2011, Published online June 29, 2011)